

# Two Microtubule-associated Proteins Required for Anaphase Spindle Movement in *Saccharomyces cerevisiae*

David Pellman,\*‡ Molly Bagget,\* Huei Tu,\* and Gerald R. Fink\*

\*The Whitehead Institute for Biomedical Research, Cambridge, Massachusetts 02142; and ‡Department of Hematology/Oncology, The Dana-Farber Cancer Institute and The Children's Hospital, Boston, Massachusetts 02115

**Abstract.** In many eucaryotic cells, the midzone of the mitotic spindle forms a distinct structure containing a specific set of proteins. We have isolated *ASE1*, a gene encoding a component of the *Saccharomyces cerevisiae* spindle midzone. Strains lacking both *ASE1* and *BIK1*, which encodes an *S. cerevisiae* microtubule-associated protein, are inviable. The analysis of the phenotype of a *bik1 ase1* conditional double mutant suggests that *BIK1* and *ASE1* are not required for the assembly of a bipolar spindle, but are essential for anaphase spindle elon-

gation. The steady-state levels of *Ase1p* are regulated in a manner that is consistent with a function during anaphase: they are low in G1, accumulate to maximal levels after S phase and then drop as cells exit mitosis. Components of the spindle midzone may therefore be required in vivo for anaphase spindle movement. Additionally, anaphase spindle movement may depend on a dedicated set of genes whose expression is induced at G2/M.

**M**ITOSIS is achieved by sequential structural changes in the mitotic spindle. The centrosomes or microtubule organizing centers duplicate, a bipolar spindle is assembled, and then at anaphase, sister chromosomes are distributed to opposite poles so that each daughter cell receives a complete chromosome set. Anaphase is divided into two stages, anaphase A, when the chromosomes move to the spindle poles, and anaphase B, when the spindle is extended and the poles are segregated between mother and daughter cells. The typical mitotic spindle has three classes of microtubules: polar microtubules that extend from the centrosomes and interdigitate with polar microtubules from the opposite pole, kinetochore microtubules that connect chromosomes to the centrosome, and astral microtubules that radiate away from the spindle into the cytoplasm and to the cell cortex. The ordered changes in spindle structure are proposed to be determined primarily by proteins that bind along the length and at the ends of microtubules (23, 46, 50). These microtubule-associated proteins (MAPs)<sup>1</sup>, are thought to act either by regulating the polymerization of tubulin, or as "motors," microtubule-based mechanochemical enzymes (30, 65).

Experimental evidence supports two contrasting mechanisms for anaphase pole separation—a pushing mecha-

nism (the poles are pushed apart by forces generated from the central spindle), and a pulling mechanism (the poles are pulled apart by forces acting on astral microtubules) (5, 42). The idea of a pushing force is supported by three-dimensional electron microscopic reconstructions of mitotic spindles from a variety of organisms (17, 42, 47). During anaphase, polar microtubules increase in length and the region of overlap between polar microtubules decreases (in varying degrees in different organisms). This finding suggests that polar microtubules polymerize and slide past each other in the midzone of the spindle. Additional evidence for a pushing mechanism comes from experiments showing that the central spindle of diatoms and *Schizosaccharomyces pombe* can elongate in vitro in the absence of astral microtubules (14, 43). Evidence for a pulling force comes from the observation in *Fusarium* that the rate of separation of the poles is increased by breaking the central spindle (1), and in vertebrate epithelial cells, that the centrosomes continue to separate after their microtubule arrays no longer overlap (72).

The spindle midzone plays an important role in both the pushing and pulling models. In many organisms, the spindle midzone undergoes a dramatic morphological transformation during anaphase (17, 42, 48). Polar microtubules, which are initially distributed randomly throughout the central spindle, become organized into regular geometric arrays, with microtubules from one pole lying adjacent to microtubules from the opposite pole. This high degree of organization is likely to be imposed by the protein components of the spindle midzone. In animal cells, the spindle midzone is surrounded by an electron-dense material that has been termed the stem body matrix (18). A

Address correspondence to Gerald R. Fink, The Whitehead Institute for Biomedical Research, Cambridge, MA 02142. Tel.: (617) 258-5215. Fax: (617) 258-9872.

1. *Abbreviations used in this paper:* DAPI, 4,6-diamidino-2-phenylindole; HU, hydroxyurea; MAP, microtubule-associated protein; SPB, spindle pole body.

number of animal cell proteins have now been identified that localize to the spindle midzone at specific stages of the cell cycle (18, 53). Although information about the in vivo function of these proteins is limited, several functions have been suggested. In models where the poles are pushed apart, the spindle midzone is envisioned to have a role in generating the forces that drive anaphase B. In models where the poles are pulled apart, the midzone proteins are thought to serve as a guide to orient spindle movement and limit its rate (5, 42).

The ability to isolate mutations affecting mitosis in *Saccharomyces cerevisiae* has provided a key link to the in vivo function of spindle proteins in centrosome duplication, spindle assembly, and kinetochore function (54). Mutant analysis supports pushing forces exerted by polar microtubules as the primary mechanism for anaphase spindle elongation in *S. cerevisiae* (68). A cold-sensitive allele of *TUB2*, the gene encoding  $\beta$ -tubulin, polymerizes nuclear (containing both polar and kinetochore microtubules) but not cytoplasmic microtubules. Spindle elongation and nuclear division occur, but the spindle is misoriented, and nuclear division takes place entirely within the mother cell. This result suggests that in *S. cerevisiae*, cytoplasmic microtubules are required to orient the spindle with the plane of cell division, but that the nuclear microtubules generate the forces for anaphase spindle elongation.

Despite the extensive characterization of yeast mitotic mutants, none encoding a spindle protein that is required primarily for anaphase spindle elongation has yet been described. A good candidate for a protein involved in anaphase pole movement is the nonmotor MAP encoded by the *BIK1* gene (8). The *BIK1* gene product colocalizes with the nuclear spindle (8). *bik1* null mutants are viable, but exhibit defects in several microtubule-dependent functions such as, chromosome segregation, nuclear migration, and karyogamy (8, 70). The structure of Bik1p is similar to that of a human MAP, CLIP-170 (or restin) (9, 57). At the NH<sub>2</sub> terminus, both proteins contain copies of a 40-amino acid peptide motif found in a number of MAPs. The mi-

cro-tubule binding domain of CLIP-170 is at the NH<sub>2</sub> terminus and requires this peptide motif for microtubule binding (57). In both proteins the NH<sub>2</sub>-terminal domain is followed by a region of heptad repeats, and then a COOH-terminal domain containing a zinc-binding motif termed the CCHC box.

To determine the role of *BIK1* in mitosis, mutations showing synthetic lethality with a *bik1* null mutation were isolated. One of the genes isolated in this screen, *ASE1* (anaphase spindle elongation) encodes a new *S. cerevisiae* MAP that localizes to the midzone of the anaphase spindle. Like one human spindle midzone protein, Ase1p levels are low in G1 but accumulate during mitosis (11). Analysis of strains deficient in *BIK1* and *ASE1* function indicates that these genes are essential for anaphase spindle elongation.

## Materials and Methods

### Strains and Microbial Techniques

Media and genetic techniques were as described in Sherman et al. (66). Yeast plasmids and linear DNA fragments for gene replacement were transformed into yeast by lithium acetate transformation (34). The mating pheromone,  $\alpha$ -factor was added to log phase cultures in synthetic complete media to a final concentration of 6  $\mu$ g/ml for 3–4 h until >80% of the cells had arrested with an unbudded shmoo morphology. To release cells from  $\alpha$ -factor arrest, cells were collected by filtration, washed, and resuspended in fresh media. Hydroxyurea was added directly to cultures in synthetic complete media to a final concentration of 0.1 M for ~4 h until >80% of cells had a large budded morphology. Lists of yeast strains and plasmids used in this study are provided in Tables I and II.

### Genetic Techniques

The *ADE3* sectoring assay and the strains for the synthetic lethality screen have been described (7, 36). *MAT $\alpha$  bik1::TRP1 ade2 ade3* strains were transformed with a *BIK1 URA3 ADE3* 2 $\mu$  plasmid. *ade2 ade3* strains are white but *ade2 ADE3* strains accumulate a red pigment. Because *BIK1* is not an essential gene, the *BIK1 ADE3 URA3* plasmid will be lost during growth on nonselective medium. This results in colonies that are red but contain white sectors that are the result of plasmid loss. Strains that con-

Table I. Yeast Strains Used in This Study

Strain	Genotype	Source of Reference
Y382	<i>MAT<math>\alpha</math> ade2 ade3 ura3 leu2 trp1</i>	Bender and Pringle, 1991
Y383	<i>MAT<math>\alpha</math> ade2 ade3 ura3 leu2 trp1 lys2</i>	Bender and Pringle, 1991
Y388	<i>MAT<math>\alpha</math> ade2 ade3 ura3 leu2 lys2</i>	Bender and Pringle, 1991
PY434	<i>MAT<math>\alpha</math> bik1-1::TRP1 ade2 ade3 ura3 leu2 trp1</i>	This study
PY435	<i>MAT<math>\alpha</math> bik1-1::TRP1 ade2 ade3 ura3 leu2 trp1 lys2</i>	This study
PY446	<i>MAT<math>\alpha</math> bik1-1::TRP1 ade2 ade3 ura3 leu2 trp1</i> {pDP58}	This study
PY452	<i>MAT<math>\alpha</math> bik1-1::TRP1 ade2 ade3 ura3 leu2 trp1 lys2</i> {pDP58}	This study
PY523	<i>MAT<math>\alpha</math> bik1-1::TRP1 ade2 ade3 ura3 leu2 trp1 lys2</i>	This study
PY582	<i>MAT<math>\alpha</math> ase1-1 bik1-1::TRP1 ade2 ade3 ura3 leu2 trp1 lys2</i> {pDP58}	This study
PY688	<i>MAT<math>\alpha</math> bik1-1::TRP1 ade2 ade3 ura3 leu2 trp1 lys2</i> {pDP140}	This study
PY945	<i>MAT<math>\alpha</math>/MAT<math>\alpha</math> ade2/ade2 ade3/ade3 ura3/ura3 leu2/leu2 lys2/LYS2 trp1/TRP1</i>	This study
PY968	<i>MAT<math>\alpha</math> ase1<math>\Delta</math>1::URA3 ade2 ade3 ura3 leu2</i>	This study
PY989	<i>MAT<math>\alpha</math> ase1<math>\Delta</math>1::URA3 ade2 ade3 ura3 leu2</i> {pDP300}	This study
PY1011	<i>MAT<math>\alpha</math> ase1-1 bik1-1::TP1 ade2 ade3 ura3 leu2 trp1 lys2</i> {pDP58}	This study
PY1012	<i>MAT<math>\alpha</math> ASE1 BIK1 ade2 ade3 ura3 leu2 trp1 lys2</i> {pRS315}	This study
PY1013	<i>MAT<math>\alpha</math> ase1-1 bik1-1::TRP1 ade2 ade3 ura3 leu2 trp1 lys2</i> {pDP65}	This study
PY1014	<i>MAT<math>\alpha</math> ase1-1 bik1-1::TRP1 ade2 ade3 ura3 leu2 trp1 lys2</i> {pDP93}	This study
PY1045	<i>MAT<math>\alpha</math> bik1-1::TRP1 ade2 ade3 ura3 leu2 trp1 lys2</i> {pDP93}	This study
PY1085	<i>MAT<math>\alpha</math>/MAT<math>\alpha</math> ade2/ade2 ade3/ade3 ura3/ura3 leu2/leu2 lys2/LYS2 trp1/TRP1</i> {pRS315}	This study
PY1088	<i>MAT<math>\alpha</math>/MAT<math>\alpha</math> ase1-1/ase1-1 bik1-1::TRP1/bik1-1::TRP1 ade2/ade2 ade3/ade3 ura3/ura3 leu2/leu2 lys2/LYS2 trp1/trp1</i> {pDP93}	This study

Table II. Plasmids Used in This Study

Plasmid	Description	Source or Reference
pRS315	<i>CEN LEU2</i> yeast shuttle vector	Sikorski and Hieter, 1989
PRS305	<i>LEU2</i> yeast integrating vector	Sikorski and Hieter, 1989
YCplac111	<i>CEN LEU2</i> yeast shuttle vector	Gietz and Sugino, 1988
pVB20	<i>BIK1 URA3</i> 2 $\mu$	Berlin et al., 1990
PKK-1	A 177-bp fragment encoding three copies of the myc tag in pUC119	D. Kornitzer and S. Kron (Whitehead Institute, Cambridge, MA)
pDP58	A 3.7-kb BamHI-NheI fragment containing <i>ADE3</i> cloned into the BamHI-NheI sites of pVB20	This study
pDP65	A 3-kb EcoRI-HindIII fragment of <i>BIK1</i> cloned into pRS315	This study
pDP93	A derivative of pDP65 containing <i>bik1-S419</i>	This study
pDP140	5-kb SacI-NsiI fragment containing <i>ASE1</i> cloned into the SacI-PstI sites of pRS305	This study
pDP243	A 3.9-kb SacI-BamHI fragment containing <i>ASE1</i> in pRS315	This study
pDP275	A plasmid for one step disruption of <i>ASE1</i>	This study
pDP300	A derivative of pDP243 containing <i>ASE1</i> tagged with three tandem copies of the myc epitope	This study
pMA1071	<i>CEN LEU2</i> vector with a 10.5-kb insert containing <i>CIN1</i>	A. Hoyt (Johns Hopkins Univ., Baltimore, MD)
pTH25	pRS305 with a 4.3-kb fragment containing <i>TUB2</i>	T. Huffaker (Cornell Univ., Ithaca, NY)
pJS47	<i>CEN LEU2</i> vector with a 3.1-kb insert containing <i>TUB1</i>	P. Schatz and F. Solomon (M.I.T., Cambridge, MA)

tain mutations that are lethal in combination with *bik1* are identified because they require the *BIK1 ADE3 URA3* plasmid for viability and will therefore have a nonsectoring red colony phenotype. The inclusion of *URA3* on the plasmid allows an independent test for plasmid loss (10).

*bik1::TRP1 ade2 ade3* strains containing the *BIK1 URA3 ADE3* 2 $\mu$  plasmid were mutagenized with ethylmethane sulfonate to give 30% survival (38). Approximately 40,000 mutagenized colonies were plated at 30°C and nonsectoring red colonies were isolated. Colonies were tested for growth on synthetic complete media containing 5-fluoro-orotic acid (10). To determine if the nonsectoring phenotype was due to a requirement for *BIK1*, mutant colonies were transformed with a *BIK1* plasmid that did not have the *ADE3* gene. From 91 candidates, 12 recessive mutants were identified that depended specifically on the *BIK1* gene for viability. Four of these mutant strains were complemented for the nonsectoring red colony phenotype by plasmids containing *TUB1*, *TUB2*, or *CIN1* and were not studied further. The remaining mutants were crossed with a *bik1::TRP1 ade2 ade3* strain to demonstrate that the mutation represented a single genetic locus and to obtain *MATa* mutant strains for complementation analysis. Diploids created by the crossing of haploid single mutants were tested for the mutant phenotypes. Mutants were assigned to the same complementation group if doubly heterozygous diploids had the nonsectoring red colony phenotype. The eight mutant strains were found to be in three complementation groups (five alleles in one group-*ASE1*, two alleles in another, and one allele in a third).

To isolate the *ASE1* gene, a *LEU2-CEN* library (no. 77162; American Type Culture Collection, Rockville, MD) was introduced into a nonsectoring *ase1-1* strain. Plasmids were recovered from sectoring colonies. Many of the plasmids contained the *BIK1* gene, and one contained a fragment that was not *BIK1*. The putative *ASE1* genomic fragment was introduced into a *LEU2*-containing yeast integrating plasmid and the resulting plasmid was transformed into an *ade2 ade3 leu2* strain. Southern analysis confirmed that integration of the putative *ASE1* fragment created a duplication of this genomic locus marked with *LEU2*. This strain was then crossed to an *ase1-1 leu2* strain and the resulting diploids were sporulated. All of the 33 four-spore tetrads segregated 2 *ASE1 LEU2*: 2 *ase1 leu2* indicating that this genomic clone contained the *ASE1* locus.

The chromosomal location of the *ASE1* gene was determined by hybridization of an *ASE1* probe to separated chromosomes and to a set of ordered  $\lambda$  phage clones (59). The *ASE1* probe hybridized to chromosome 15 and to a single  $\lambda$  clone,  $\lambda$ 6030.

A deletion of *ASE1*, *ase1 $\Delta$ 1::URA3*, was created by replacing the DNA segment encoding amino acids 1–858 with a DNA fragment containing the selectable marker *URA3*. The deletion construct, *ase1 $\Delta$ 1::URA3*, was transformed into an *ade2/ade2 ade3/ade3 ura3/ura3 leu2/leu2 trp1/TRP1* diploid yeast strain. Stable *Ura<sup>+</sup>* transformants were selected and analyzed by Southern blot to confirm that the transformants were heterozygous for the disruption of the *ASE1* gene. The *ASE1/ase1 $\Delta$ 1::URA3* diploids were sporulated and tetrads were dissected. In greater than 90% of

the tetrads all four spores germinated. In four spore tetrads, *URA3* segregated 2 to 2 with *Ura<sup>+</sup>* spores found with equal frequency to *Ura<sup>-</sup>* spores. The deletion of the *ASE1* gene was also confirmed by southern analysis of *Ura<sup>+</sup>* spores.

To determine if the deletions of *BIK1* and *ASE1* showed synthetic lethality, an *ASE1/ase1 $\Delta$ 1::URA3 BIK1/bik1-1::TRP1* diploid was sporulated and tetrads dissected. From 30 tetrads, no *Trp<sup>+</sup>Ura<sup>+</sup>* (*bik1 ase1*) progeny were recovered though *ase1 $\Delta$ 1::URA3* and *bik1-1::TRP1* single mutant spores were identified at the expected frequency.

### DNA Manipulations

DNA cloning was done as outlined in Sambrook et al. (62). The *BIK1 ADE3 URA3* 2m plasmid (pDP58) was constructed by cloning a 3677 bp BamHI-NheI fragment containing *ADE3* into a *BIK1 URA3* 2 $\mu$  plasmid, pVB20 (8).

For sequencing *ASE1*, a 10.5-kb fragment containing *ASE1* was cloned in both orientations into a *LEU2 CEN* plasmid (YCplac111) (24). Nested deletions of these plasmids were made using exonuclease ExoIII and nuclease S1 (29). Deletions were tested for complementation and the sequence of both strands of a 3,901-bp complementing fragment was determined. Double-stranded dideoxy sequencing with Sequenase (United States Biochemical, Cleveland, OH) was performed. The sequence was edited using the Lasergene software package (DNASTAR, London, UK) and analyzed using UWGCG programs (16). The probability that regions of *Ase1p* form a coiled-coil structure was determined by the algorithm of Lupas et al. (40) using a 28-amino acid window size. Data base searches were performed using BLAST (3). The sequence of the *ASE1* locus has been submitted to the GenBank data base (accession number 420235).

The 3,901-bp SacI-BamHI fragment of *ASE1* was subcloned into the yeast shuttle vector pRS315 (67) and into a derivative of pUC119 lacking the EcoRI site in the polylinker (pDP 243 and pDP259, respectively).

The null allele *ase1 $\Delta$ 1::URA3* contains a deletion corresponding to amino acids 1–858. Nucleotides 748–3362 were replaced with a BglII linker and a 5-kb cassette containing *URA3* was introduced at this site (pDP275) (2).

Site-directed mutagenesis of *BIK1* and *ASE1* was performed by the technique of Kunkel (37). The *bik1-S419* allele, which has a change of cysteine to serine at amino acid 419 was constructed with an oligonucleotide of sequence 5'-GTGAGCATTCCGATACCATGGGTC-3'. Three tandem copies of the myc tag were introduced into the coding sequence of *ASE1* in two steps. By site-directed mutagenesis, a unique NheI site was introduced after nucleotide 3526 that is after the codon for the last amino acid of *Ase1p*. An oligonucleotide of sequence 5'-GGATTCCTTTA-CAGATATTGCTAGCATTTCCTAAAAGCGC-3' was used. An XbaI fragment containing the coding sequence for three tandem copies of the myc tag was then introduced into this NheI site (D. Kornitzer and S. Kron, unpublished observation). The epitope-tagged *ASE1* fully complements

the nonsectoring phenotype of *ase1* strains. In addition, a different strain (W303) than the one used for the studies (7) described in this paper has a weak temperature-sensitive growth defect when the *ASE1* gene is deleted. The epitope-tagged *ASE1* complements the growth defect in this strain.

### Microscopic Analysis of Cells

To examine cell morphology cell cultures were stained with 4,6-diamidino-2-phenylindole (DAPI). Microtubule structures were observed after fixation in formaldehyde with the rat anti-tubulin antibody, YOL1/34 (58). Spindle pole bodies were observed after fixation for 5 min at 24°C in formaldehyde with a mixture of mAbs against a 90-kD SPB protein (61, 63). To visualize the intracellular location of Ase1p marked with the epitope tag, cells were double labeled YOL1/34 and the 9E10 mAb directed against the myc epitope. Fluorochrome-conjugated secondary antibodies were from Jackson ImmunoResearch Labs., Inc. (West Grove, PA). For double labeling, control experiments demonstrated that cross-species reactivity did not contribute to the final images when species-specific secondary antibodies were used. These experiments also demonstrated that light channel spill-over did not contribute to the final images. For quantitative analysis greater than 200 consecutive cells were counted.

Cells were prepared for thin-section electron microscopy by a modification of the procedure of Byers and Goetsch (13). Glutaraldehyde fixed cells were digested in 0.02 mg/ml Oxalyticase (Enxogenetics, Corvallis, OR) and Glusulase (Du Pont NEN, Boston, MA) at a dilution of 1/10 in 0.17 M KH<sub>2</sub>PO<sub>4</sub>, 30 mM sodium citrate, and 0.03 M 2-mercaptoethanol until the majority of cells had become spheroplasts as determined by phase microscopy. Spheroplasts were post-fixed with 2% osmium tetroxide in 0.05 M sodium acetate, pH 6.1, and en block stained with 1% aqueous uranyl acetate at 4°C overnight. Samples were dehydrated in graded ethanol and embedded in polyBed 812 (Polysciences, Inc., Warrington, PA). Thin sections were collected on 75 mesh pioloform (Ted Pella, Inc., Irvine, PA). Samples were examined with a Phillips EM410 microscope at 60 kV. To determine the percentage of *bik1 ase1* cells that had splayed microtubules consecutive fields were scanned for cells with short spindles. These were then qualitatively assessed to have normal or splayed microtubules.

### Flow Cytometry

Yeast strains were grown to early log phase at 24°C, collected by filtration and resuspended at 36°C. The cells were fixed with 70% ethanol for 30 min at 24°C. Cells were stained with propidium iodide as described (33). Stained cells were analyzed on a FACSTAR (Becton Dickinson Immunocytometry Sys., Mountain View, CA) using LYSIS II version 1.2. Cell sorting was performed based on the flow cytometry profile. Sorted cells were collected, restrained with propidium iodide, and nuclear morphology was examined by epifluorescence.

### Western and Northern Blot Analysis

Cells were prepared for Western blotting by vortexing for 3 min with an equal volume of glass beads in buffer containing 50 mM TRIS, pH 7.5, 1 mM EDTA, 5% 2-mercaptoethanol and protease inhibitors. Extracts were then boiled in Laemmli sample buffer and the amount of Ase1p and  $\beta$ -tubulin in 50  $\mu$ g of total cell protein was determined by an enhanced chemiluminescence detection system (Amersham Corp., Arlington Heights, IL). Epitope-tagged Ase1p was detected with 9E10 mAb.  $\beta$ -tubulin was detected with a polyclonal antibody (a gift from F. Solomon, M.I.T., Cambridge, MA). Total cell RNA was prepared for northern blot analysis using the method of Elion and Warner (19). A DNA probe containing the coding sequence from the *H2B1* locus for northern analysis was isolated by PCR from yeast genomic DNA. The primers used for PCR were of sequence: 5'-GAC-AAGTCAAACCAATAAACC-3' and 5'-TGCTTGAGTAGAG-GAAGAGTA-3'.

## Results

### Isolation of Mutations That Are Lethal in a *bik1* Null Strain

Because *bik1* null strains are viable, we screened for mutations that are lethal in combination with a *bik1* null allele. Such mutations were expected to identify other spindle components with overlapping or dependent functions (25).

Mutants were isolated and characterized as described in the Materials and Methods. 12 recessive mutations were found that showed synthetic lethality with a *bik1* null allele. Four of the mutants were found to be in genes whose function had been shown previously (8) to be required for viability in *bik1* strains (the tubulin genes, *TUB1* and *TUB2*, and the *CINI* gene that is required for accurate chromosome segregation and microtubule stability, 31). The identification of alleles of these genes validates our experimental approach to identifying new spindle-associated proteins whose function is required in a *bik1* mutant. Complementation analysis demonstrated that the remaining mutants defined three genes (five alleles in one group, two alleles in another, and one allele in a third). One locus (five alleles) was termed *ASE1* for anaphase spindle elongation because of the phenotype of a *bik1 ase1* double mutant (see subsequent sections).

### Isolation and Sequence Analysis of *ASE1*

The *ASE1* gene was isolated by complementation of an *ase1* strain using a plasmid library. Targeted integration was used to establish that the cloned fragment contains the *ASE1* gene (see Materials and Methods). The chromosomal location of the *ASE1* gene was determined by hybridization of an *ASE1* probe to separated chromosomes and to a mapped yeast DNA library. *ASE1* is on the right arm of chromosome 15 ~100 kb from the centromere (see Materials and Methods).

Sequence analysis of the *ASE1* locus revealed that the *ASE1* open reading frame is predicted to encode an 885-amino acid protein with an unmodified molecular mass of 102 kD and an estimated pI of 9.80 (GenBank accession number 420235). Ase1p is predicted to have an  $\alpha$ -helical secondary structure throughout most of the length of the protein (22, data not shown). Two short regions (amino acids 142–171 and amino acids 493–527) of Ase1p are predicted to have a probability of greater than 0.8 of forming a coiled-coil structure by the method of Lupas et al. (40). Data base searches revealed low level homology to many proteins that have a coiled-coil  $\alpha$ -helical structure. Although Ase1p does not have homology to known microtubule-associated proteins, the basic pI and regions predicted to form a coiled-coil structure are common features of MAPs from other organisms.

### A Null Allele of *ASE1* Is Viable

A deletion of *ASE1* lacking the coding sequence for amino acids 1–858 was created by homologous recombination (see Materials and Methods). Strains carrying the *ase1* deletion showed no difference from *ASE1* strains when analyzed for the following phenotypes: growth rate, temperature sensitivity, and unilateral and bilateral karyogamy defects. However, like *bik1* strains, the *ase1* strain is moderately supersensitive to the microtubule depolymerizing drug benomyl (the *ase1* strain has a growth defect at 5  $\mu$ m/ml as compared to 15  $\mu$ m/ml for the isogenic control). To determine the phenotype of a strain containing deletions of both *BIK1* and *ASE1*, a *MAT $\alpha$  ase1* null strain was crossed to a *MAT $\alpha$  bik1* null strain. No double mutant progeny were recovered from this cross indicating that the *ase1* deletion allele, like the *ase1* alleles isolated in our

screen, shows synthetic lethality with a *bik1* null mutant (see Materials and Methods).

### *Ase1p Has a Novel Localization on the Mitotic Spindle*

A simple explanation for the lethality of *bik1 ase1* double mutants would be that *ASE1* encodes a MAP that performs a similar function to Bik1p. To test this hypothesis, the intracellular location of Ase1p was determined by immunolocalization of a fully functional epitope-tagged Ase1p (see Materials and Methods). Three tandem copies of a DNA sequence encoding a peptide epitope from the myc protein (21) were introduced into the COOH-terminal coding sequence of *ASE1*. A centromere-based plasmid containing epitope-tagged *ASE1* was then transformed into an *ase1* null strain. An asynchronous culture of this

strain was fixed and stained with two mAbs, one directed against tubulin and the other against the myc epitope. The localization of Ase1p in cells in different stages of the cell cycle was visualized by indirect immunofluorescence (Fig. 1). In G1 cells that only contain astral microtubule structures, no specific staining of Ase1p is observed (Fig. 1, A–C). In cells that contain short bipolar spindles, Ase1p shows clear localization along the mitotic spindle (Fig. 1, D–F). Little or no staining is observed at the ends of the spindle corresponding to the region of the spindle pole bodies (the yeast centrosomes). In cells that have completed anaphase with segregated DNA and long spindles (telophase), Ase1p staining is restricted to an  $\sim 2\text{-}\mu\text{m}$  bar at the midzone of the spindle (Fig. 1, G–I). This pattern of localization was observed in almost all cells examined. 98% of cells with G1 astral microtubules ( $n = 200$ ) had no

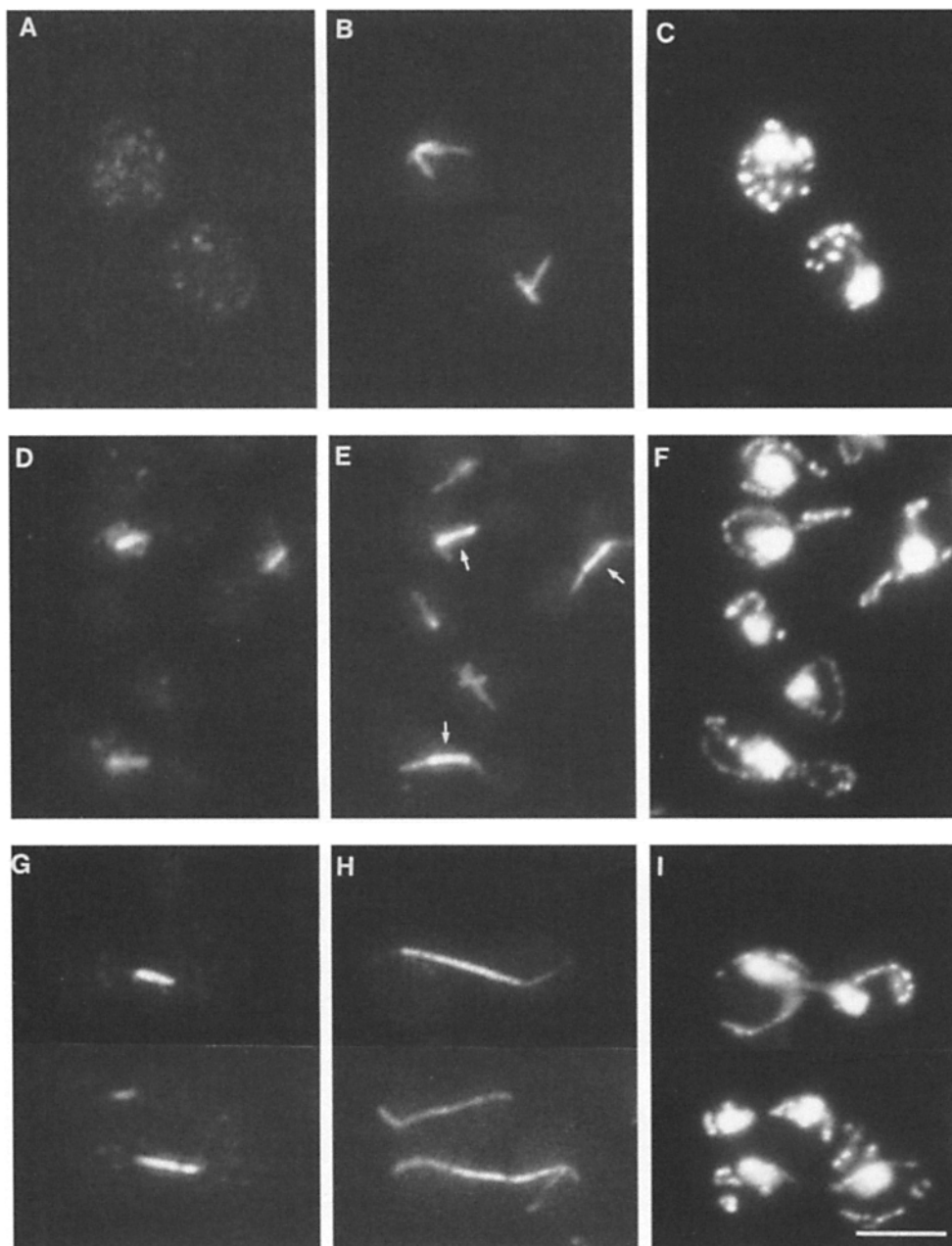


**Figure 1.** Intracellular localization of epitope-tagged Ase1p. The photographs are from an asynchronous culture containing epitope-tagged Ase1p on a centromere-based plasmid. (A–C) Two G1 cells. (D–F) Three S/G2 cells with short bipolar spindles. (G–I) Three anaphase/telophase cells. (A, D, and G) Cells stained with 9E10, an  $\alpha$ -myc antibody recognizing epitope-tagged Ase1p. The cells were stained with a CY3-conjugated goat anti-mouse secondary antibody and visualized with rhodamine fluorescence. (B, E, and H) Cells stained with Yoll/34 an anti-tubulin mAb. The cells were stained with a fluorescein isothiocyanate-conjugated secondary antibody and visualized with fluorescein isothiocyanate fluorescence. (C, F, and I) DAPI staining of DNA to visualize nuclei. Control experiments with an isogenic strain carrying *ASE1* plasmid lacking the epitope tag showed no staining. Bar, 5  $\mu\text{m}$ .

specific staining of Ase1p. 92% of cells with short bipolar spindles ( $n = 231$ ) showed staining of Ase1p on the nuclear microtubules, and 97% of cells with long spindles and segregated DNA ( $n = 206$ ) showed Ase1p staining at the midzone of the spindle.

### Multiple Centrosomes in Strains Lacking *BIK1* and *ASE1* Function

The lethality of *bik1 ase1* double mutants and the viability of the single null mutants indicates that either gene can perform a function that is essential for viability. To determine the essential function missing in the double mutant, we created a conditional (temperature sensitive) *bik1 ase1* strain whose defects could be analyzed at the nonpermissive temperature. The desired double mutant was identified by combining several in vitro constructed alleles of *BIK1* with the five alleles of *ASE1* isolated in the screen for synthetic lethality with *bik1*. One double mutant, *bik1-S419 ase1-1*, has a strong recessive temperature-sensitive growth defect. The *bik1-S419 ase1-1* strain has a modest growth defect at 24 and 30°C but does not grow at 36°C. The *bik1-S419* allele encodes a point mutation in the COOH-terminal zinc binding motif of Bik1p. The *bik1-S419* mutation is a partial loss of function allele because *bik1-S419 tub1-1* double mutants have a growth defect (but are viable) and because strains carrying *bik1-S419* have a partial karyogamy defect (data not shown). The *bik1-S419 ase1-1* strain will hereafter be referred to as *bik1 ase1*.

The *bik1 ase1* strain exhibits dramatic defects in spindle morphology at the nonpermissive temperature. *bik1 ase1* and *BIK1 ASE1* strains were grown at 24°C, shifted to 36°C, fixed, and then prepared for indirect immunofluorescence. *BIK1 ASE1* strains show characteristic microtubule structures representing all stages of the yeast cell cycle: G1 asters, S/G2 short bipolar spindles, and long anaphase/telophase spindles (Fig. 2, A and B). By contrast, the *bik1 ase1* strain displays three classes of abnormal microtubule structures (Fig. 2, C and D): large budded cells with very short (less than 1  $\mu\text{m}$ ) bipolar spindles, budded cells with single spindle poles, and budded or unbudded cells with multiple short spindles and multiple spindle

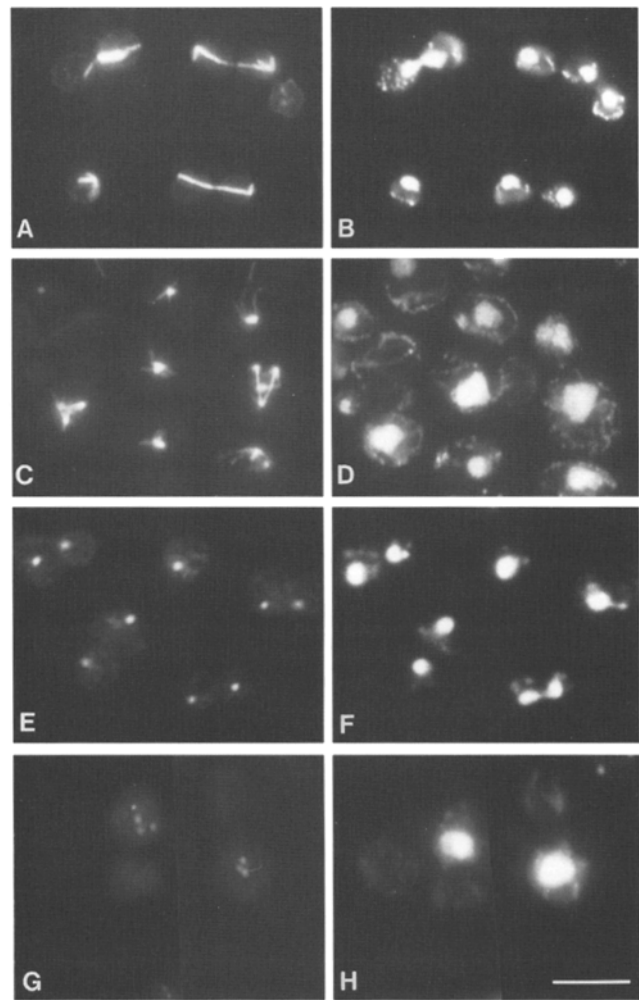


**Figure 2.** Multiple centrosome phenotype of the *bik1 ase1* strain at 36°C. (A, B, E, and F) Control *BIK1 ASE1* strain 6 h at 36°C. (C, D, G, and H) *bik1 ase1* strain 6 h at 36°C. (A and C) Microtubules stained with the YOL1/34 anti-tubulin mAb. (E and G) SPBs stained with mAbs against the 90-kD SPB protein. (B, D, F, and H) DAPI staining of DNA to visualize nuclei. Bar, 10  $\mu\text{m}$ .

**Table III. Cell and Spindle Morphology of *bik1-S419* and *ase1-1* Single and Double Mutants**

	<i>BIK1 ASE1</i>	<i>bik1-S419 ASE1</i>	<i>BIK1 ase1-1</i>	<i>bik1 ase1 ts</i>
	46	38	17	8
	0	0	19	13
	38	41	42	24
	16	0	6	2
	0	19	10	0
	0	0	2	20
	0	2	4	34

Cultures of *BIK1 ASE1*, *bik1-S419 ASE1*, *BIK1 ase1-1*, and *bik1 ase1 ts* strains were shifted to 37°C for 6 h and examined by anti-tubulin immunofluorescence and DAPI staining. The percentage of cells with the morphologies shown on the left were determined by counting greater than 200 cells. From top to bottom, the following classes of cells were seen: unbudded cells with a single spindle pole, budded cells with single spindle poles, budded cells with short bipolar spindles, post-anaphase cells with long spindles and segregated DNA, post-anaphase cells with broken spindles, either unbudded or budded cells with multiple spindle poles in a single nucleus, and anucleate cells.

poles. These three classes of spindle structures are observed in approximately equal numbers in the *bik1 ase1* strain (Table III). The finding that the *bik1 ase1* strain accumulates cells with multiple spindle pole bodies (SPB) was confirmed by staining with a mixture of monoclonal antibodies against the 90-kD spindle pole body component (61), (Fig. 2, G and H). Although it was not possible to photograph more than three spindle pole bodies in a single focal plane, most cells with more than two SPBs appeared to have four SPBs when the entire cell was examined by changing focal planes. A small percentage of cells appeared to have more than four SPBs, but the exact number of poles in these cells was difficult to determine because of the overlap of adjacent poles. Perhaps the most notable feature of the *bik1 ase1* strain at 36°C is the absence of post-anaphase cells with long spindles and segregated DNA (two foci of DAPI staining material).

Microtubules in *bik1-S419* and *ase1-1* single mutant

strains were examined by indirect immunofluorescence (Table III). The spindle structures in the *bik1-S419* strain are indistinguishable from the *BIK1 ASE1* strain. The microtubule structures in the *ase1-1* strain had abnormalities similar to the *bik1 ase1* strain but were less dramatic and less frequent. Many large budded cells had short bipolar spindles. Additionally, there were large budded cells with single poles, and rare cells with multiple SPBs.

The *bik1 ase1* strain was examined by transmission electron microscopy (Fig. 3). In wild-type yeast cells, the SPB is composed of a trilaminar structure and the spindle is formed from arrays of microtubules emanating from the opposite SPBs (12; Fig. 3 A). In the *bik1 ase1* strain at 36°C the SPBs had a normal morphology, but microtubule structures were abnormal. In *bik1 ase1* cells with short bipolar spindles, the microtubules from opposite poles appeared splayed (Fig. 3 B), suggesting that *BIK1* and *ASE1* may be required to maintain the organization of anti-parallel microtubules. The frequency of the splayed spindle structure was 75% when consecutive cells ( $n = 24$ ) with short spindles were examined. In the cells with single spin-

dle poles, duplicated SPBs were found adjacent to each other (Fig. 3 C).

#### **Cells lacking *BIK1* and *ASE1* Assemble Bipolar Spindles, but Fail to Elongate the Spindle during Anaphase**

A culture of the *bik1 ase1* strain was synchronized in G1 at the permissive temperature and then shifted to the non-permissive temperature to determine when the first observable defects in cell division occur. A *MATa bik1 ase1* strain and wild-type control were synchronized in G1 with  $\alpha$ -factor at 24°C. Cell cultures were then released from this block into fresh media at 36°C and samples were removed at times after release and examined by phase microscopy and fluorescence microscopy for tubulin distribution. Progression into the cell cycle was measured by scoring the percentage of cells with large buds and the percentage of cells containing both segregated DNA and long spindles spanning the length of the mother and daughter cells (telophase cells). In the *BIK1 ASE1* strain, cells progress normally into the cell cycle after release from an  $\alpha$ -factor

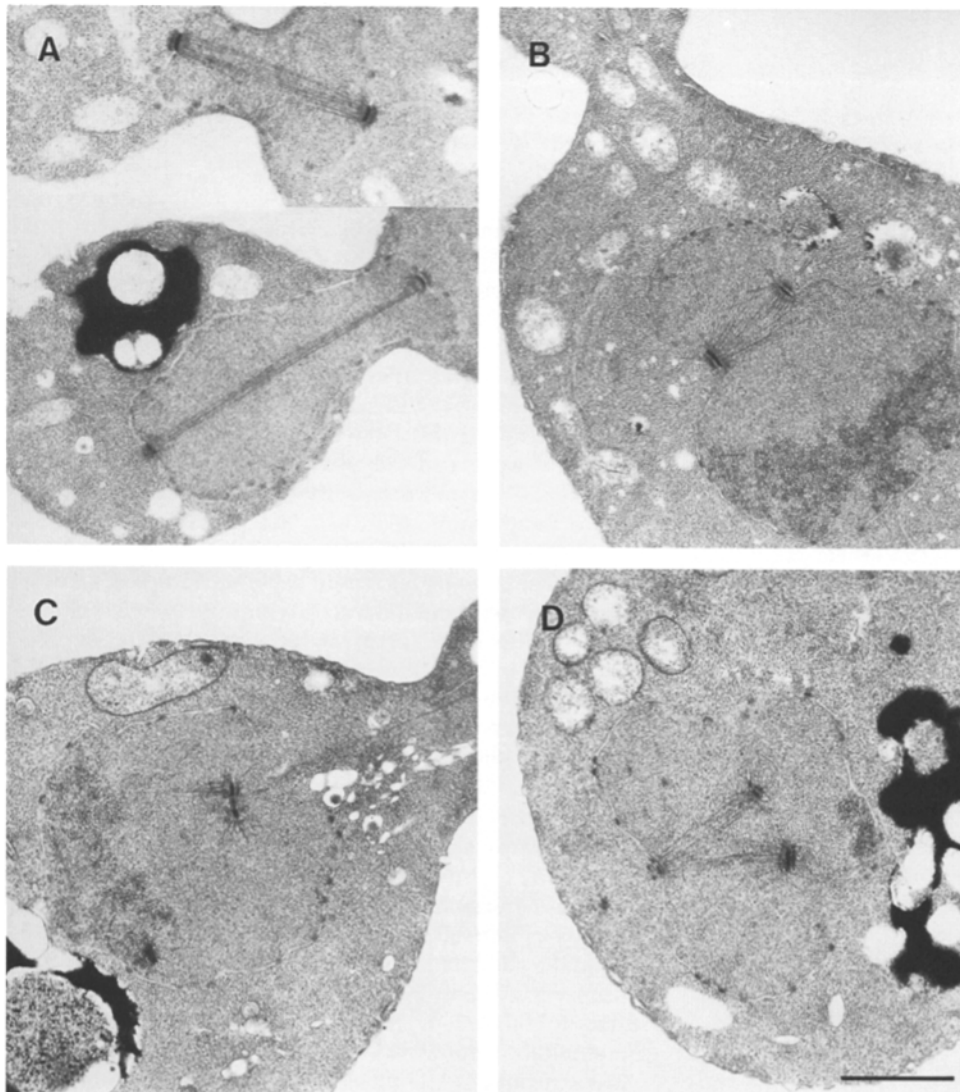
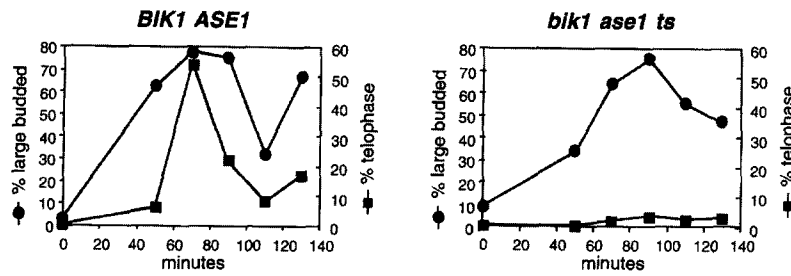
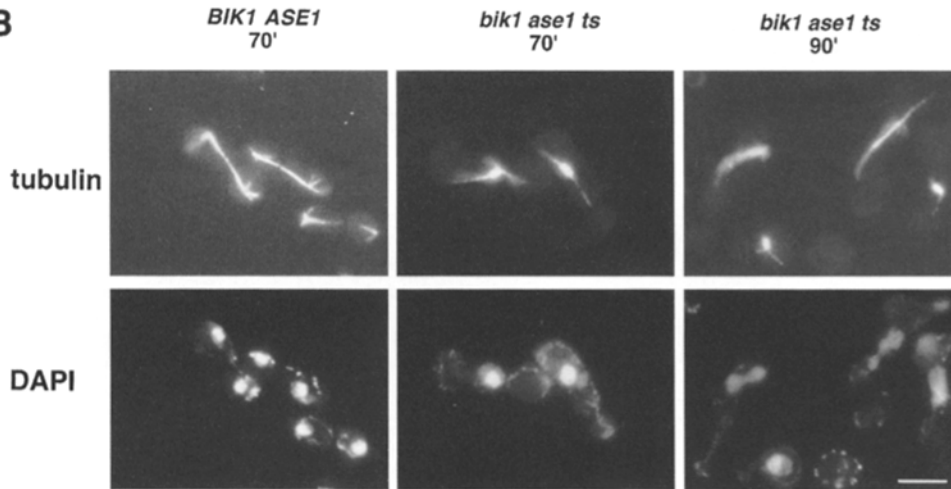


**Figure 3.** Electron microscopic analysis of *BIK1 ASE1* and *bik1 ase1* cells. Cells were prepared for electron microscopy after a 4-h shift to 36°C. (A) Two *BIK1 ASE1* cells. (B) A *bik1 ase1* cell with a short spindle exhibiting splayed microtubules. (C) A *bik1 ase1* cell with a single pole having two side by side SPBs. (D) A *bik1 ase1* cell with three SPBs in the plane of the section. Bar, 1  $\mu$ m.

**A**



**B**



130', 3%, 64%, 17%, 15%. (B) Spindle structures in synchronized *BIK1 ASE1* and *bik1 ase1* cells. The top panels show microtubule structures visualized with anti-tubulin antibodies, and the bottom panels show DNA stained with DAPI. Two cells from the *bik1 ase1* strain (top, far right) demonstrate defective anaphase spindles. Bar, 5  $\mu$ m.

block. Dividing cells form large buds around the time of bipolar spindle assembly and remained with large buds until cytokinesis (Fig. 4 A).

In the *bik1 ase1* strain, mitosis is uncoupled from bud growth and cytokinesis (Fig. 4 A). Although the *bik1 ase1* strain initiates and completes budding with similar kinetics as the *BIK1 ASE1* control, *bik1 ase1* cells assembled bipolar spindles, but fail to complete anaphase normally (Fig. 4 B). After release from  $\alpha$ -factor, when mothers and daughters are roughly the same size, wild-type cells have completed anaphase, but the *bik1 ase1* cells (85%) have short spindles and an undivided nucleus. After longer periods at the nonpermissive temperature, a percentage (15%) of *bik1 ase1* cells show highly defective anaphase spindle structures, with very short anaphase spindles and nuclear division occurring entirely within the mother cell (Fig. 4 B, 90 min).

$\alpha$ -Factor block and release experiments performed with a single mutant *bik1-S419* strain gave similar results to those performed with the *BIK1 ASE1* strain. After release from  $\alpha$ -factor, the majority of single mutant *ase1-1* cells complete anaphase but do so more slowly than the control strain. Some cells showed spindles defects reminiscent of those seen in *bik1 ase1* cells (data not shown).

#### Loss of *BIK1* and *ASE1* Function During S Phase Does Not Destroy the Bipolar Spindle or Alter the Subsequent Mitosis

Experiments were performed to test whether *BIK1* and

*ASE1* are required during S phase, when the bipolar spindle is assembled (12). Yeast cells treated with the DNA synthesis inhibitor, hydroxyurea (HU), arrest in S phase as large budded cells with an undivided nucleus and a short spindle. If *BIK1* and *ASE1* were required to maintain spindle pole separation in cells arrested with hydroxyurea, then the spindle would be predicted to collapse after a shift to the nonpermissive temperature. *bik1 ase1* and control strains were arrested with HU at the permissive temperature (24°C), and then shifted for 1.5 h to the nonpermissive temperature (36°C) in the presence of HU. At 24°C both strains arrest with short spindles (96% of *BIK1 ASE1* cells; 84% of *bik1 ase1* cells). After 1.5 h at 36°C both strains remained arrested with intact short spindles (98% of *BIK1 ASE1* cells; 83% of *bik1 ase1* cells). Although we do not know precisely how rapidly *BIK1* and *ASE1* function is lost in the *bik1 ase1* strain at 36°C, marked defects in spindle structure were observed at 36°C 70 min after release from a G1 block (Fig. 4 B). Therefore, incubation at 36°C for 1.5 h should have been sufficiently long to observe an effect. Under similar conditions, the spindle collapses in strains such as *cin8-3 kip1 $\Delta$*  (63) that have a defect in spindle assembly.

Loss of *BIK1* and *ASE1* function might result in a defect in S phase, but this defect might not be observable until later in the cell cycle. This hypothesis was tested by the following experiment. *bik1 ase1* and control cells were arrested in HU at 24°C. The cells were then split into three samples. One sample was shifted to 36°C for 1.5 h and then released from the HU block at 24°C. Another sample was

Figure 4. Defective anaphase spindle elongation in *bik1 ase1* cells. Indirect immunofluorescence was obtained with anti-tubulin antibodies of a *BIK1 ASE1* strain and a *bik1 ase1* strain after release at 36°C from an  $\alpha$ -factor block at 24°C. (A) The percentage of large budded cells (circles) was scored by phase microscopy and the percentage of telophase cells (segregated DNA and spindles extending the length of the mother and daughter cells, squares) was scored by fluorescence microscopy. The spindle morphologies observed in large budded cells after release from the G1 block were, telophase, bipolar short spindles, monopolar spindles, and defective anaphase. The percentages of large budded *bik1 ase1* cells with these morphologies at the timepoints after release were, respectively: 50', 3%, 84%, 10%, 2%; 70', 2%, 85%, 11%, 3%; 90', 4%, 70%, 11%, 15%; 110', 1%, 66%, 18%, 17%;



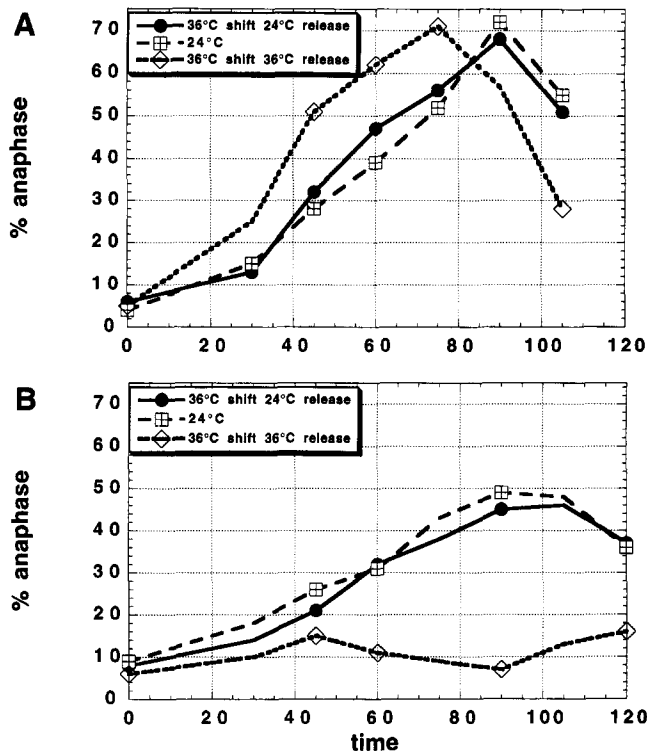


**Figure 5.** Loss of *BIK1* and *ASE1* function during S phase does not block subsequent anaphase. Early exponential cultures of control *BIK1ASE1* (A) and *bik1 ase1* double mutant (B) strains were arrested in S phase with 0.1 M hydroxyurea for 4 h. Each culture was then split. Closed circles indicate cells that were shifted to 36°C for 1.5 h in HU, washed and then released at 24°C. Sectioned squares indicate cells that were maintained at 24°C throughout the experiment. Open squares indicate cells that were shifted to 36°C for 1.5 h in HU, washed and then released at 36°C. Cells were collected at intervals for DAPI staining and the percentage of cells that successfully completed anaphase were identified as large-budded cells with two separate masses of DAPI-staining material.

shifted to 36°C for 1.5 h and then released from the HU block at 36°C. The final sample was maintained in HU at 24°C for 1.5 h and then released from the HU block at 24°C. The percentage of cells that completed anaphase, as reflected by successful nuclear division, was then scored by DAPI staining. Fig. 5 B shows that a 1.5-h temperature shift during S phase does not affect the subsequent mitosis when *bik1 ase1* cells are released at 24°C. These experiments suggest that the *bik1 ase1* double mutant does not have an S phase defect.

#### Loss of *BIK1* and *ASE1* Function Uncouples Mitosis from Cytokinesis and DNA Replication

Despite the defect in mitosis, the *bik1 ase1* strain at 36°C does not undergo arrest with a uniform terminal phenotype (Table III). After a 6-h shift to 36°C, both budded and unbudded cells are present in roughly equal proportions. A significant proportion of the unbudded cells are anucleate. The proportion of anucleate cells that were observed in this experiment is comparable to the proportion of cells with multiple spindle pole bodies (Table III), con-

sistent with the idea that these two cell types result from division of the same parent cell. The finding that the number of anucleate cells is slightly greater than the number of cells with multiple SPBs is likely to be due to multiple rounds of division by cells with multiple SPBs. The fact that the strain fails to undergo cell cycle arrest is also confirmed by the fact that in synchronized cells at the nonpermissive temperature the percentage of large budded cells decreases with time (Fig. 4 A).

To test the hypothesis that the *bik1 ase1* strain continues DNA replication despite the block in nuclear division, the DNA content of a homozygous *bik1 ase1* temperature-sensitive diploid strain was measured at 36°C by flow cytometry. By contrast with a wild-type diploid strain (Fig. 6 A), the double mutant accumulates two abnormal populations of cells, a hypoploid population and a hyperploid population (Fig. 6 B). Microscopic examination of cells isolated from the hypoploid peak by fluorescence-activated cell sorting showed that these cells were unbudded anucleate cells. Flow cytometry of the double mutant at 24°C also identified hypoploid and hyperploid peaks that were smaller than the peaks observed from cultures at 36°C. This finding is consistent with the growth defect of the double mutant at the permissive temperature. The homozygous double mutant, therefore, accumulates anucleate cells and cells with increased DNA content.

#### Cell Cycle-specific Accumulation of *Ase1p*

One explanation for the absence of immunofluorescence staining for *Ase1p* in G1 cells is that there is less *Ase1p* in these cells (Fig. 1). The steady state levels of *Ase1p* were therefore examined in synchronized cells after release from a G1 block with  $\alpha$ -factor. Samples were collected at intervals for phase microscopy, Western blot, and Northern blot analysis. Cell cycle position was assessed by cell morphology and by the level of histone (H2B) mRNA. H2B transcripts reach maximal levels at the G1/S boundary and then decline at the end of S phase (28). *Ase1p* is not detectable in cells arrested with  $\alpha$ -factor but then increases to maximal levels after the decline of H2B mRNA

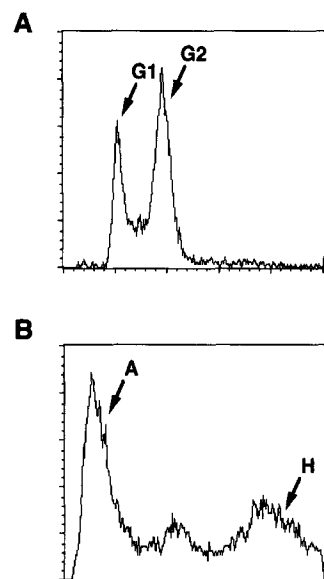


**Figure 6.** DNA content of *bik1 ase1* and control cells at 36°C. (A) A diploid *BIK1/ASE1* strain after a 6 h shift to 36°C. (B) A homozygous *bik1 ase1* diploid strain after 6 h at 36°C. Fixed cells were stained with propidium iodide and analyzed by flow cytometry. Fluorescence intensity is indicated on the X axis. Cell number is indicated on the Y axis. After the 6-h shift the *bik1 ase1* strain accumulates anucleate cells (peak A) and a hyperploid population of cells (peak H).

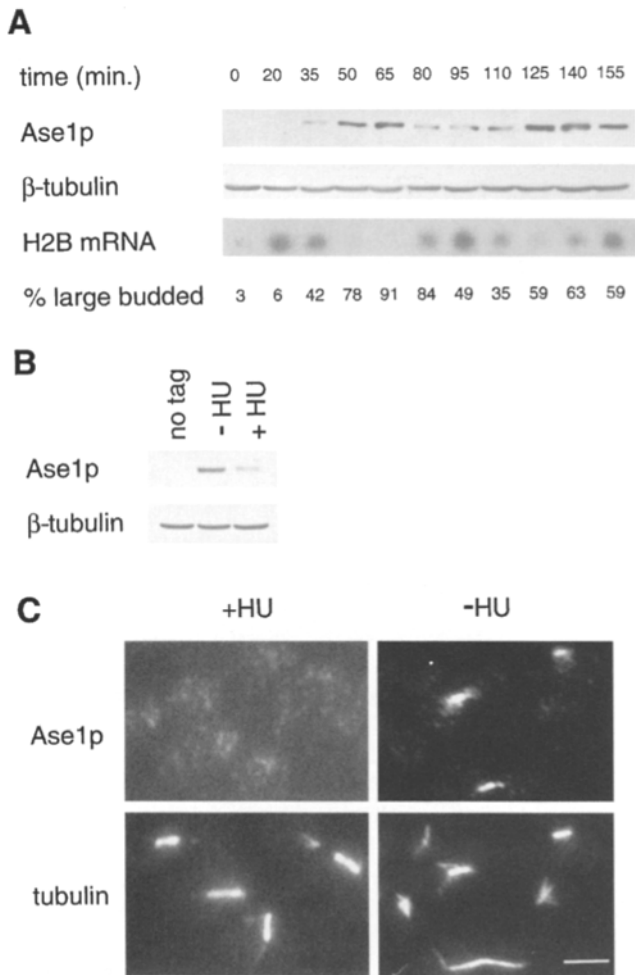


**Figure 7.** Ase1p accumulates after S phase. (A) Cell cycle changes in the steady state levels of Ase1p. A strain carrying epitope-tagged *ASE1* on a centromere plasmid was arrested in G1 with  $\alpha$ -factor. Cells were released from the  $\alpha$ -factor block at 30°C and aliquots were removed at the indicated times for analysis of cell morphology, Ase1p and  $\beta$  tubulin levels, and H2B RNA levels. (B) Comparison of Ase1p levels in exponentially growing cells and in cells arrested in S phase with hydroxyurea. An isogenic control strain containing an *ASE1* plasmid lacking the epitope is included to show the specificity of the  $\alpha$ -myc antibody for epitope-tagged Ase1p. (C) Comparison of Ase1p localization in exponentially growing cells and in cells arrested in S phase with hydroxyurea. The top panels show Ase1p localization detected with  $\alpha$ -myc antibody. The bottom panels show tubulin staining detected with YOL1/34. Bar, 5  $\mu$ m.

when cells have developed large buds. Ase1p levels then decline as cells exit mitosis and undergo cytokinesis (Fig. 7 A). Because the *S. cerevisiae* bipolar spindle is assembled during S phase (12), Ase1p probably does not reach maximal levels until after spindle assembly. An independent test of this conclusion was performed by examining Ase1p levels and localization in cells arrested with HU. Cells arrested with HU have significantly reduced levels of Ase1p relative to cells from an asynchronous culture (Fig. 7 B). Furthermore, indirect immunofluorescence shows that Ase1p is not associated with the spindle in HU-arrested cells (Fig. 7 C). These experiments suggest that Ase1p be-

comes a significant component of the bipolar spindle only after S phase.

## Discussion

### An *S. cerevisiae* Component of the Midzone of the Anaphase Spindle

Using a screen for mutations that show synthetic lethality with *BIK1*, we have identified *ASE1*, which encodes a component of the midzone of the *S. cerevisiae* anaphase spindle. The association of Ase1p with microtubules varies during the cell cycle. In G1 cells there is no Ase1p staining on astral microtubules, in S/G2 cells, Ase1p staining is seen along the nuclear microtubules of short spindles, and in late anaphase/telophase cells the Ase1p staining is restricted to an  $\sim 2$ - $\mu$ m bar in the midzone of the spindle. The extent of the midzone staining corresponds to the extent of overlap between polar microtubules during anaphase in *S. cerevisiae* (73).

The absence of Ase1p staining in G1 cells can be attributed to cell cycle changes in steady state levels of Ase1p. Ase1p is not detectable in G1 cells arrested with  $\alpha$ -factor, but accumulates to maximal levels after the decline of H2B mRNA at the end of S phase. Since the bipolar spindle in *S. cerevisiae* is assembled late in S phase (12), it is likely that Ase1p accumulates after spindle assembly. This interpretation is further supported by the fact that Ase1p levels are low, and do not show detectable association with the bipolar spindle of cells arrested with the DNA synthesis inhibitor, HU.

The variation in the levels of Ase1p is due, at least in part, to changes in the steady state level of the *ASE1* mRNA. The level of the *ASE1* transcript oscillates in a similar manner to the messages for B-type cyclins and other G2/M-specific transcripts (D. Pellman, unpublished results). Furthermore, it is likely that *ASE1* is coordinately regulated with these other G2/M-specific transcripts. The *ASE1* promoter (-287- -251: tcccaatgaggtaaaaggtaaataa) contains an element that binds MCM1 and a factor termed SFF that is found in the promoters of several G2/M-regulated transcripts (35, 41).

One other fungal protein, *S. pombe cut7*, which encodes a protein related to the microtubule-based motor, kinesin, is associated with the spindle midzone (26, 27). Unlike Ase1p, *cut7* is also strongly associated with the spindle poles. Temperature-sensitive mutants of *S. pombe cut7* are defective in spindle assembly. Because the *cut7* gene product localizes to the spindle poles in addition to the central spindle, the defect in spindle assembly could reflect *cut7* function at either or both sites.

In view of the functional overlap between *BIK1* and *ASE1*, one might expect colocalization of Ase1p and Bik1p. The interpretation of the experiments on Bik1p localization is complicated by the fact that we have been able to detect Bik1p by immunofluorescence only when it is overexpressed approximately 10-fold from a 2 $\mu$  plasmid. When overexpressed, Bik1p is not associated with microtubules in G1 cells but is observed along the entire length of the spindle (nuclear microtubules) during mitosis (reference 8 and D. Pellman, unpublished results). Failure to observe restricted localization of Bik1p to the spindle mid-

zone could be a consequence of overexpression. Indeed, when Ase1p is expressed from a 2 $\mu$  plasmid, we observe staining along the entire length of the spindle rather than the clear demarcation of the midzone observed when Ase1p is expressed from a low copy number plasmid (D. Pellman, unpublished results).

### The *bik1 ase1* Mutant Has a Defect in Anaphase B

The simplest hypothesis to explain the phenotype of the *bik1 ase1* strain at 36°C is that the growth limiting defect in this strain is in spindle elongation. The mutant phenotypes can then be explained by the following model. The *bik1 ase1* strain can duplicate the SPB normally and establish a short (metaphase-like) bipolar spindle. However, this bipolar spindle is defective and fails to elongate, resulting in failure of nuclear division. If there is no cell cycle arrest, subsequent cytokinesis will produce an anucleate cell and an unbudded cell with two SPBs. This "G1" cell with two SPBs will reinitiate the cell cycle resulting in a cell with four SPBs and increased DNA content (diagrammed in Fig. 8).

The hypothesis that *bik1 ase1* is defective in spindle elongation is supported by the analysis of the spindle morphology of cells at the nonpermissive temperature. After release from a G1 block, the earliest point in mitosis that the *bik1 ase1* mutant exhibits a spindle defect is after the assembly of a bipolar spindle. Although *bik1 ase1* cells form bipolar spindles, these structures are abnormally short and the microtubules appear splayed. The double mutant therefore manifests a functional defect in anaphase, where spindle elongation either does not occur or is markedly abnormal. The fact that the *bik1 ase1* strain does not undergo cell cycle arrest and undergoes abnormal spindle elongation supports the idea that spindle elongation itself is defective and not simply entry into anaphase.

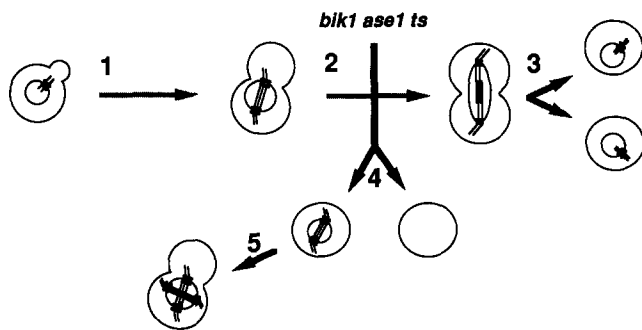


**Figure 8.** Defect in the *bik1 ase1* double mutant. The model presents the proposed stage of mitosis that is defective in the *bik1 ase1* strain. Microtubules are represented by thin lines and the spindle pole bodies are represented by thick lines. The nuclear envelope is represented by circles or ovals contained within the cells. Note that the *S. cerevisiae* nuclear envelope does not break down during mitosis. The gray arrows and numbers 1 through 3 indicate normal stages of the *S. cerevisiae* cell cycle. Black arrow and numbers 4 and 5 represent proposed abnormal cell cycle stages in the *bik1 ase1* strain. (1) SPB duplication and spindle assembly. (2) Anaphase spindle elongation. (3) Nuclear division and cytokinesis. (4) Cytokinesis in the absence of nuclear division in the *bik1 ase1* strain. (5) The cell from stage 4 goes through an additional cell cycle to produce a cell with multiple centrosomes.

The conclusion that *bik1 ase1* cells are able to form bipolar spindles is supported by several observations. First, 85% of *bik1 ase1* cells form bipolar spindles after release at the nonpermissive temperature from a G1 block. Second, *bik1 ase1* cells arrested in HU maintain bipolar spindles even after prolonged incubation at the nonpermissive temperature. Finally, loss of *bik1 ase1* function in HU-arrested cells does not prevent subsequent anaphase when cells are released from the S phase block at the permissive temperature. Because bipolar spindle structure is abnormal in *bik1 ase1* cells (Fig. 3 B), we suggest that *BIK1* and *ASE1* are required after the bipolar spindle is assembled to establish structures required for anaphase.

These experiments suggest that the *bik1 ase1* double mutant is defective in anaphase. However, we cannot exclude the possibility that either Bik1p or Ase1p has an additional role at an earlier stage of mitosis. For example, there could be a defect in the rate of spindle assembly that is not obvious in our experiments analyzing timepoints from fixed samples of cells. A delay in spindle assembly could be inferred from the fact that a proportion of *bik1 ase1* cells at the nonpermissive temperature have monopolar spindles. However, note that synchronized cells at the nonpermissive temperature accumulate monopolar spindles after the majority of cells have formed bipolar spindles (see Fig. 4 legend). At least a portion of the *bik1 ase1* cells with monopolar spindles may therefore arise by spindle collapse after spindle assembly. A role in some other aspect of mitosis is perhaps more likely for *BIK1* because *BIK1* is expressed throughout the cell cycle (D. Pellman, unpublished results). The expression of *ASE1* only after the spindle is assembled makes it unlikely that Ase1p is required earlier in the cell cycle.

One other *S. cerevisiae* mutant, *esp1-1* has a multiple spindle pole body phenotype similar to that of the *bik1 ase1* mutant (6, 45). *esp1* cells fail to elongate short spindles and progress through the cell cycle with similar kinetics to wild-type cells (45, 69). Mutations in related genes from other fungi result in similar phenotypes (44, 71). Based on our analysis of *bik1 ase1* cells and on the analysis of *esp1* cells by McGrew et al. (45), we suggest that the accumulation of multiple spindle bodies is a signature phenotype for a defect in anaphase B in *S. cerevisiae*.

### Anaphase Spindle Elongation in *Saccharomyces*

Genetic experiments in *S. cerevisiae* have suggested a role for both pushing and pulling forces on the spindle poles during anaphase. Our experiments support the view that a pushing force generated by nuclear microtubules is of primary importance. Yeast strains with deletions of the genes encoding the cytoplasmic dynein heavy chain (20, 39), or candidate light chains (15, 49, 51), are viable and undergo anaphase B. However, these mutants are defective in orienting the spindle with the plane of cell division and, therefore, produce a significant number of cells with a binucleate phenotype. These results have been interpreted to suggest that pulling forces generated from cytoplasmic microtubules are important for spindle orientation, but make only a minor contribution to anaphase B.

Although the binucleate phenotype has been taken to indicate a defect in the function of cytoplasmic microtu-

bules, it is also possible that this phenotype could be produced by a defect in nuclear microtubules. Because nuclear migration is dynamic, with extensive movement of the nucleus and rotation of the spindle before anaphase (reference 55 and J. Kahana and P. Silver, personal communication), a delay in spindle elongation relative to the timing of cytokinesis could produce binucleate cells. In fact, one of the most striking mitotic defects in *bik1* strains is the accumulation of binucleate and anucleate cells (8). The colocalization of Bik1p with nuclear microtubules supports the hypothesis that the binucleate phenotype of *bik1* strains results from a defect in nuclear microtubule function.

Proteins associated with nuclear microtubules are the obvious candidates for generating a pushing force on the poles. Aside from Bik1p and Ase1p, several *S. cerevisiae* proteins have been isolated that localize to nuclear microtubules, two kinesin-like proteins, Cin8p and Kip1p (32, 60), and one non-motor MAP, Stu1p (56). The phenotype of the *bik1 ase1* strain is strikingly different from strains containing mutations in these genes. Strains lacking *STU1* or *CIN8* and *KIP1* display marked defects in spindle assembly. *CIN8* and *KIP1* are also required to maintain the structure of short bipolar spindles in cells arrested in S phase with HU (63). In addition to their function early in mitosis, recent experiments suggest that Cin8p and Kip1p also contribute to anaphase spindle movement. A triple mutant, lacking the function of *CIN8*, *KIP1* and *DYNI*, is defective in anaphase B (64). Coordinated spindle movement may therefore require both proteins whose function is required throughout mitosis, such as Cin8p and Kip1p, as well as proteins whose function is restricted to specific stages of mitosis.

### The Spindle Midzone During Anaphase

Evidence from animal cells suggests that the spindle midzone may be a distinct sub-organelle composed of a unique set of proteins (18). The phenotype of the *bik1 ase1* mutant suggests that in vivo the spindle midzone plays a critical role in anaphase B. We have considered two possible functions for Bik1p and Ase1p. First, these proteins may be components of a filamentous matrix associated with the spindle (4, 18, 52). This matrix could regulate microtubule polymerization, organize microtubules from opposite poles, or provide a scaffold for microtubule-based motors to generate movement of microtubules during spindle elongation. Alternatively, either Bik1p or Ase1p could be a subunit of a microtubule-based motor.

Our finding that Bik1p and Ase1p are required after the time at which the spindle is formed supports the view that mitosis is driven by the ordered assembly and functioning of spindle-associated proteins. Furthermore, the regulated pattern of Ase1p expression suggests that anaphase is not simply a continuation of the process of spindle assembly, but requires the function of dedicated genes. The identification of *ASE1* from *S. cerevisiae* should facilitate the isolation of other regulated components of the anaphase spindle and help to reveal the mechanism by which the spindle midzone functions during anaphase.

We thank J. Loeb and other members of the Fink laboratory for stimulating discussions. We thank A. Bender, J. Kilmartin, D. Kornitzer, S. Kron,

J. Loeb, and F. Solomon, for generously providing strains and reagents. A. Amon, J. Loeb, M. McLaughlin, and P. Silver provided comments on the manuscript. We are grateful to G. Paradis and L. Vaught for flow cytometry and cell sorting. We thank C. Y. Tai and P. Grisafi for technical assistance. D. Pellman acknowledges the support of S. Lux.

This work was supported by a Pediatric Scientist Development Award and an National Institutes of Health Clinical Investigator Award to D. Pellman and National Institutes of Health grants GM-35010 and GM-40266 to G. R. Fink.

Received for publication 17 May 1995 and in revised form 6 June 1995.

### References

1. Aist, J. R., and M. W. Berns. 1981. Mechanics of chromosome separation during mitosis in *Fusarium* (Fungi imperfecti): new evidence from ultrastructural and laser microbeam experiments. *J. Cell Biol.* 91:446-458.
2. Alani, E., L. Cao, and N. Kleckner. 1987. A method for gene disruption that allows repeated use of URA3 selection in the construction of multiply disrupted yeast strains. *Genetics.* 116:541-545.
3. Altschul, S. F., W. Gish, W. Miller, E. W. Myers, and D. J. Lipman. 1990. Basic local alignment search tool. *J. Mol. Biol.* 215:403-410.
4. Andreassen, P. R., D. K. Palmer, M. H. Wener, and R. L. Margolis. 1991. Telophase disc: a new mammalian mitotic organelle that bisects telophase cells with a possible function in cytokinesis. *J. Cell Sci.* 99:523-534.
5. Ault, J. G., and C. L. Rieder. 1994. Centrosome and kinetochore movement during mitosis. *Curr. Opin. Cell Biol.* 6:41-49.
6. Baum, P., C. Yip, L. Goetsch, and B. Byers. 1988. A yeast gene essential for regulation of spindle pole duplication. *Mol. Cell Biol.* 8:5386-5397.
7. Bender, A., and J. R. Pringle. 1991. Use of a screen for synthetic lethal and multicopy suppressor mutants to identify two new genes involved in morphogenesis in *Saccharomyces cerevisiae*. *Mol. Cell Biol.* 11:1295-1305.
8. Berlin, V., C. A. Styles, and G. R. Fink. 1990. BIK1, a protein required for microtubule function during mating and mitosis in *Saccharomyces cerevisiae*, colocalizes with tubulin. *J. Cell Biol.* 111:2573-2586.
9. Bilbe, G., J. Delabie, J. Bruggen, H. Richener, F. Asselbergs, N. Cerletti, C. Sorg, K. Odink, L. Tarcsay, W. Wiesendanger, C. De Wolf-Peters, and R. Shipman. 1992. Restin: a novel intermediate filament-associated protein highly expressed in the Reed-Sternberg cells of Hodgkin's disease. *EMBO J.* 11:2103-2113.
10. Boeke, J. D., J. Trueheart, G. Natsoulis, and G. R. Fink. 1987. 5-Fluoroorotic acid as a selective agent in yeast molecular genetics. *Methods Enzymol.* 154:164-175.
11. Brown, K. D., R. M. Coulson, T. J. Yen, and D. W. Cleveland. 1994. Cyclin-like accumulation and loss of the putative kinetochore motor CENP-E results from coupling continuous synthesis with specific degradation at the end of mitosis. *J. Cell Biol.* 125:1303-1312.
12. Byers, B. 1981. Cytology of the yeast life cycle. In *The Molecular Biology of the Yeast Saccharomyces: Life Cycle and Inheritance*. J. N. Strathern, E. W. Jones, and J. R. Broach, editors. Cold Spring Harbor Laboratory, Cold Spring Harbor, New York. 59-96.
13. Byers, B., and L. Goetsch. 1974. Duplication of spindle plaques and integration of the yeast cell cycle. *Cold Spring Harbor Symp. Quant. Biol.* 38:123-131.
14. Cande, W. Z., and K. L. McDonald. 1985. In vitro reactivation of anaphase spindle elongation using isolated diatom spindles. *Nature (Lond.)* 316:168-170.
15. Clark, S. W., and D. I. Meyer. 1994. *ACT3*: a putative centractin homologue in *S. cerevisiae* is required for proper orientation of the mitotic spindle. *J. Cell Biol.* 127:129-138.
16. Devereux, J., P. Haeberli, and O. Smithies. 1984. A comprehensive set of sequence analysis programs for the VAX. *Nucleic Acids Res.* 12:387-395.
17. Ding, R., K. L. McDonald, and J. R. McIntosh. 1993. Three-dimensional reconstruction and analysis of mitotic spindles from the yeast, *Schizosaccharomyces pombe*. *J. Cell Biol.* 120:141-151.
18. Earnshaw, W. C., and A. M. Mackay. 1994. Role of nonhistone proteins in the chromosomal events of mitosis. *FASEB J.* 8:947-956.
19. Elion, E. A., and J. R. Warner. 1984. The major promoter element of rRNA transcription in yeast lies 2 kb upstream. *Cell.* 39:663-673.
20. Eshel, D., L. A. Urrestarazu, S. Vissers, J. C. Jauniaux, J. C. van Vliet-Reedijk, R. J. Planta, and I. R. Gibbons. 1993. Cytoplasmic dynein is required for normal nuclear segregation in yeast. *Proc. Natl. Acad. Sci. USA.* 90:11172-11176.
21. Evan, G. I., G. K. Lewis, G. Ramsay, and J. M. Bishop. 1985. Isolation of monoclonal antibodies specific for human c-myc proto-oncogene product. *Mol. Cell Biol.* 5:3610-3616.
22. Garnier, J., D. J. Osguthorpe, and B. Robson. 1978. Analysis of the accuracy and implications of simple methods for predicting the secondary structure of globular proteins. *J. Mol. Biol.* 120:97-120.
23. Gelfand, V. I., and A. D. Bershadsky. 1991. Microtubule dynamics: mechanism, regulation, function. *Annu. Rev. Cell Biol.* 7:93-116.
24. Gietz, R. D., and A. Sugino. 1988. New yeast-*Escherichia coli* shuttle vec-

- tors constructed with in vitro mutagenized yeast genes lacking six-base pair restriction sites. *Gene (Amst.)*. 74:527–534.
25. Guarente, L. 1992. Synthetic enhancement in gene interaction: a genetic tool come of age. *Trends Genet.* 9:362–366.
  26. Hagan, I., and M. Yanagida. 1990. Novel potential mitotic motor protein encoded by the fission yeast *cut7+* gene. *Nature (Lond.)*. 347:563–566.
  27. Hagan, I., and M. Yanagida. 1992. Kinesin-related *cut7* protein associates with mitotic and meiotic spindles in fission yeast. *Nature (Lond.)*. 356:74–76.
  28. Hereford, L. M., M. A. Osley, J. R. Ludwig, and C. S. McLaughlin. 1981. Cell-cycle regulation of yeast histone mRNA. *Cell*. 24:367–375.
  29. Hoheisel, J., and F. M. Pohl. 1986. Simplified preparation of unidirectional deletion clones. *Nucleic Acids Res.* 14:3605.
  30. Hoyt, M. A. 1994. Cellular roles of kinesin and related proteins. *Curr. Opin. Cell Biol.* 6:63–68.
  31. Hoyt, M. A., T. A. Stearns, and D. Botstein. 1990. Chromosome instability mutants of *Saccharomyces cerevisiae* that are defective in microtubule-mediated processes. *Mol. Cell Biol.* 10:223–234.
  32. Hoyt, M. A., L. He, K. K. Loo, and W. S. Saunders. 1992. Two *Saccharomyces cerevisiae* kinesin-related gene products required for mitotic spindle assembly. *J. Cell Biol.* 118:109–120.
  33. Hutter, K. J., and H. E. Eipel. 1979. Microbial determinations by flow cytometry. *J. Gen. Microbiol.* 113:369–375.
  34. Ito, H., Y. Fukuda, K. Murata, and A. Kimura. 1983. Transformation of intact yeast cells treated with alkali cations. *J. Bacteriol.* 153:163–168.
  35. Koch, C., and K. Nasmyth. 1994. Cell cycle regulated transcription in yeast. *Curr. Opin. Cell Biol.* 6:451–459.
  36. Koshland, D., J. C. Kent, and L. H. Hartwell. 1985. Genetic analysis of the mitotic transmission of minichromosomes. *Cell*. 40:393–403.
  37. Kunkel, T. A. 1985. Rapid and efficient site-specific mutagenesis without phenotypic selection. *Proc. Natl. Acad. Sci. USA*. 82:488–492.
  38. Lawrence, C. W. 1991. Classical mutagenesis techniques. *Methods Enzymol.* 194:273–281.
  39. Li, Y. Y., E. Yeh, T. Hays, and K. Bloom. 1993. Disruption of mitotic spindle orientation in a yeast dynein mutant. *Proc. Natl. Acad. Sci. USA*. 90:10096–10100.
  40. Lupas, A., M. van Dyke, and J. Stock. 1991. Predicting coiled coils from protein sequences. *Science (Wash. DC)*. 5010:1162–1164.
  41. Lydall, D., G. Ammerer, and K. Nasmyth. 1991. A new role for MCM1 in yeast: cell cycle regulation of *SWI5* transcription. *Genes & Dev.* 5:2405–2419.
  42. Mastronarde, D. N., K. L. McDonald, R. Ding, and J. R. McIntosh. 1993. Interpolar spindle microtubules in PTK cells. *J. Cell Biol.* 123:1475–1489.
  43. Masuda, H., T. Hirano, M. Yanagida, and W. Z. Cande. 1990. In vitro reactivation of spindle elongation in fission yeast *nuc2* mutant cells. *J. Cell Biol.* 110:417–425.
  44. May, G. S., C. A. McGoldrick, C. L. Holt, and S. H. Denison. 1992. The *bimB3* mutation of *Aspergillus nidulans* uncouples DNA replication from the completion of mitosis. *J. Biol. Chem.* 267:15737–15743.
  45. McGrew, J. T., L. Goetsch, B. Byers, and P. Baum. 1992. Requirement for *ESPI* in the nuclear division of *Saccharomyces cerevisiae*. *Mol. Biol. Cell.* 3:1443–1454.
  46. McIntosh, J. R., and G. E. Hering. 1991. Spindle fiber action and chromosome movement. *Annu. Rev. Cell Biol.* 7:403–426.
  47. McIntosh, J. R., K. L. McDonald, M. K. Edwards, and B. M. Ross. 1979. Three-dimensional structure of the central mitotic spindle of *Diatoma vulgare*. *J. Cell Biol.* 83:428–442.
  48. McIntosh, J. R., U. P. Roos, B. Neighbors, and K. L. McDonald. 1985. Architecture of the microtubule component of mitotic spindles from *Dicystostelium discoideum*. *J. Cell Sci.* 75:93–129.
  49. McMillan, J. N., and K. Tatchell. 1994. The *JNMI* gene in yeast *Saccharomyces cerevisiae* is required for nuclear migration and spindle orientation during the mitotic cell cycle. *J. Cell Biol.* 125:143–158.
  50. Mitchison, T. J. 1992. Compare and contrast actin filaments and microtubules. *Mol. Biol. Cell.* 3:1309–1315.
  51. Muhua, L., T. S. Karpova, and J. A. Cooper. 1994. A yeast actin-related protein homologous to that in vertebrate dynactin complex is important for spindle orientation and nuclear migration. *Cell*. 78:669–679.
  52. Nicklas, R. B., D. F. Kubai, and T. S. Hays. 1982. Spindle microtubules and their mechanical associations after micromanipulation in anaphase. *J. Cell Biol.* 95:91–104.
  53. Nislow, C., V. A. Lombillo, R. Kuriyama, and J. R. McIntosh. 1992. A plus-end-directed motor enzyme that moves antiparallel microtubules in vitro localizes to the interzone of mitotic spindles. *Nature (Lond.)*. 359:543–547.
  54. Page, B. D., and M. Snyder. 1993. Chromosome segregation in yeast. *Annu. Rev. Microbiol.* 47:231–261.
  55. Palmer, R. E., M. Koval, and D. Koshland. 1989. The Dynamics of Chromosome Movement in the Budding Yeast *Saccharomyces cerevisiae*. *J. Cell Biol.* 109:3355–3366.
  56. Pasqualone, D., and T. C. Huffaker. 1994. *STUI*, a suppressor of a  $\beta$ -tubulin mutation, encodes a novel and essential component of the yeast mitotic spindle. *J. Cell Biol.* 127:1973–1984.
  57. Pierre, P., J. Scheel, J. E. Rickard, and T. E. Kreis. 1992. CLIP-170 links endocytic vesicles to microtubules. *Cell*. 70:887–900.
  58. Pringle, J. R., A. E. Adams, D. G. Drubin, and B. K. Haarer. 1991. Immunofluorescence methods for yeast. *Methods Enzymol.* 194:565–602.
  59. Riles, L., J. E. Dutchik, A. Baktha, B. K. McCauley, E. C. Thayer, M. P. Leckie, V. V. Braden, J. E. Depke, and M. V. Olson. 1993. Physical maps of the six smallest chromosomes of *Saccharomyces cerevisiae* at a resolution of 2.6 kilobase pairs. *Genetics*. 134:81–150.
  60. Roof, D. M., P. B. Meluh, and M. D. Rose. 1992. Kinesin-related proteins required for assembly of the mitotic spindle. *J. Cell Biol.* 118:95–108.
  61. Rout, M. P., and J. V. Kilmartin. 1990. Components of the yeast spindle and spindle pole body. *J. Cell Biol.* 111:1913–1927.
  62. Sambrook, J., E. F. Fritsch, and T. Maniatis. 1989. *Molecular Cloning: A Laboratory Manual*. Cold Spring Harbor Laboratory, Cold Spring Harbor, New York.
  63. Saunders, W. S., and M. A. Hoyt. 1992. Kinesin-related proteins required for structural integrity of the mitotic spindle. *Cell*. 70:451–458.
  64. Saunders, W. S., D. Koshland, D. Eschel, I. R. Gibbons, and M. A. Hoyt. 1995. *S. cerevisiae* kinesin- and dynein-related proteins required for anaphase chromosome segregation. *J. Cell Biol.* 128:617–624.
  65. Schroer, T. A. 1994. Structure, function and regulation of cytoplasmic dynein. *Curr. Opin. Cell Biol.* 6:69–73.
  66. Sherman, F., J. B. Hicks, and G. R. Fink. 1986. *Methods in Yeast Genetics*. Cold Spring Harbor Laboratory, Cold Spring Harbor, New York.
  67. Sikorski, R. S., and P. Hieter. 1989. A system of shuttle vectors and yeast host strains designed for efficient manipulation of DNA in *Saccharomyces cerevisiae*. *Genetics*. 122:19–27.
  68. Sullivan, D. S., and T. C. Huffaker. 1992. Astral microtubules are not required for anaphase B in *Saccharomyces cerevisiae*. *J. Cell Biol.* 119:379–388.
  69. Surana, U., A. Amon, C. Dowzer, J. McGrew, B. Byers, and K. Nasmyth. 1993. Destruction of the CDC28/CLB mitotic kinase is not required for the metaphase to anaphase transition in budding yeast. *EMBO J.* 12:1969–1978.
  70. Trueheart, J., J. D. Boeke, and G. R. Fink. 1987. Two genes required for cell fusion during yeast conjugation: evidence for a pheromone-induced surface protein. *Mol. Cell. Biol.* 7:2316–2328.
  71. Uzawa, S., I. Samejima, T. Hirano, K. Tanaka, and M. Yanagida. 1990. The fission yeast *cut1+* gene regulates spindle pole body duplication and has homology to the budding yeast *ESPI* gene. *Cell*. 62:913–925.
  72. Waters, J. C., R. W. Cole, and C. L. Rieder. 1993. The force-producing mechanism for centrosome separation during spindle formation in vertebrates is intrinsic to each aster. *J. Cell Biol.* 122:361–372.
  73. Winey, M., C. L. Mamay, E. T. O'Toole, D. N. Mastronarde, T. H. Giddings, K. L. McDonald, and J. R. McIntosh. 1995. Three-dimensional ultrastructural analysis of the *Saccharomyces cerevisiae* mitotic spindle. *J. Cell Biol.* 129:1601–1615.